CAVEAT IN FISHER'S THEOREM REVEALS FITNESS CAN CHANGE WITHOUT MUTATIONS

CARLOS REDING[1,2*]

[1] *Living Systems Institute, University of Exeter, Exeter EX4 4QD, UK.*
[2] *Department of Genetics, Stanford University. Stanford, CA 94305, USA.*

[*] **Corresponding author:** `rc_reding@teknik.io`

The fitness of microbial genotypes is linked to their reproduction rate: Mutants reproducing faster than their wild-type counterparts are favoured by selection, but otherwise the mutation is lost. Here I show that relative differences in fitness between two mutants can change over time without invoking new mutations, contravening textbook population genetics theory. Widespread fitness measurements assume the ratio between Malthusian reproduction rates of competing genotypes is constant. But they are not. Here I competed two constructs of *Escherichia coli*, one harbouring the non-transmissible plasmid pGW155B. The plasmid protects the bacterium against tetracycline, and yet, it was maintained without using the antibiotic. pGW155B imposes a slower reproduction rate due to carriage costs but it also prompts a known trade-off between reproduction and survival, so the construct harbouring pGW155B attains higher densities at the equilibrium. Consequently, if selection favours survival the bacterium could maintain the plasmid, despite its slower reproduction, without using tetracycline. Exclusive reliance on reproduction rates may therefore yield inaccurate fitness measurements, altering our intuition about how natural selection operates, unless competing genotypes reach their equilibrium. This means that selection for plasmid carriage could be stronger than previously thought.

I. INTRODUCTION

'Survival of the fittest' constitutes a central tenet in evolutionary biology, but what does '*fitness*' mean? Textbook population genetics theory (*1–3*) provides a number of formal definitions depending on different assumptions. In the simplest scenario, where a population has continuous growth and overlapping generations, fitness is defined (*2, 4*) as the population's reproductive rate given by $N(t) = N_0 e^{mt}$, where N_0 is the initial number of individuals, $N(t)$ the number of individuals at time t, and m the exponential *per capita* reproductive rate—also known as Malthusian parameter (*2, 5, 6*). While this scenario is indeed simple; compared to others that require discrete generations, age structure, or allele dominance; it is suitable to study the evolution of asexual, haploid microbial populations (*2*) and is indeed routinely used in microbiological studies (*5, 7, 8*) and included in microbiological protocols (*9*).

If fitness is an inherited trait, as it is reasonable to assume, then population genetics says that mutants with greater fitness will be represented in greater proportion in the next generation (*2*). But this rationale is problematic: It does not explain the ubiquity of trade-offs in microbes (*10*). Particularly, the case where mutants reproduce slower at the expense of higher growth yields relative to their wild-type counterpart (*10–12*). As I explain below, population genetics theory assumes that genotypes grow exponentially in haploid populations and, therefore, that relative differences in fitness are constant. Consequently, to reverse this difference mutations must occur.

The gold-standard to measure fitness in haploid genotypes (W_{ij}) is given by the ratio between *per capita* reproduction rates: $W_{ij} = m_i/m_j$ (5, 13–16). Here m is derived from the above exponential model. The underlying rationale is that mutant i will be selected *for* when $W_{ij} > 1$ and selected *against* when $W_{ij} < 1$. However, biologically speaking, it is self-evident that populations do not grow exponentially given the limited availability of resources. The Malthusian parameter m_i can be derived from the exponential growth model as $m_i = [ln(N_i(t)/N_i(0)]/t)$. As I argue below, the relative difference in fitness between genotypes using this metric depends on the time t chosen to measure $N_i(t)$. In other words, if W_{ij} is a function of time, seemingly-unfit mutants that reproduce slower can still be maintained if selection occurs at a different in time—without invoking new mutations.

To demonstrate this principle, I propagated a competition between two constructs of *Escherichia coli*, with and without a non-transmissible plasmid that protects against tetracycline. This plasmid imposes slower reproduction rate on its host, but it also prompts a known trade-off between reproduction rate and survival/carrying capacity (rK trade-off (11)). By propagating the competition at a point in time where the relative frequency of the plasmid-harbouring construct higher, it could be co-maintained without using tetracycline—despite its slower growth rate.

II. Results

Let me assume two competing genotypes, mutants A and B, that grow as consistently with population genetics theory (2). The following system of ordinary differential equations describes the change in the number of individuals of each mutant over time:

$$\begin{cases} \dot{A} = m_a A, \\ \dot{B} = m_b B, \end{cases} \tag{1}$$

where m is the Malthusian parameter as introduced above, and $A(0) = B(0) = x$ where x is strictly positive. Note that m is derived from random birth (b) and death (d) rates, so that $m = b - d$ (2), and that it is independent of the number of the number of individuals of each genotype. Each individual is equally likely to die or reproduce at any given time, and the age distribution is near to the equilibrium so that b and d are nearly constant. The growth dynamics of both mutants is illustrated in Figure 1A. In this case, as m is a constant, the relative fitness of one mutant with respect to another is also constant: $W_{ba} = m_b/m_a = k$. In other words, if $m_b = B(t)/B(0)$ and $B(t)$ is the number of individuals of mutant B at an arbitrary time t, the relative fitness W_{ba} is the same regardless of t. The same applies to the fitness of A with respect to B. Indeed, if $m_b > m_a$, the number of mutant B individuals is higher than those of mutant A at all times as Figure 1A shows.

Now suppose that m is no longer independent of the number of individuals of each genotype. This is a reasonable assumption given the depletion of resources that occurs during microbial growth, limiting the abundance of each mutant over time:

$$\begin{cases} \dot{A} = m_a\left(1 - \frac{A}{K_a}\right) A \\ \dot{B} = m_b\left(1 - \frac{B}{K_b}\right) B, \end{cases} \tag{2}$$

where K_a and K_b are the maximal population size attainable (*carrying capacity*) for mutants A and B, respectively, resulting from the limited availability of resources. Here the Malthusian parameter m

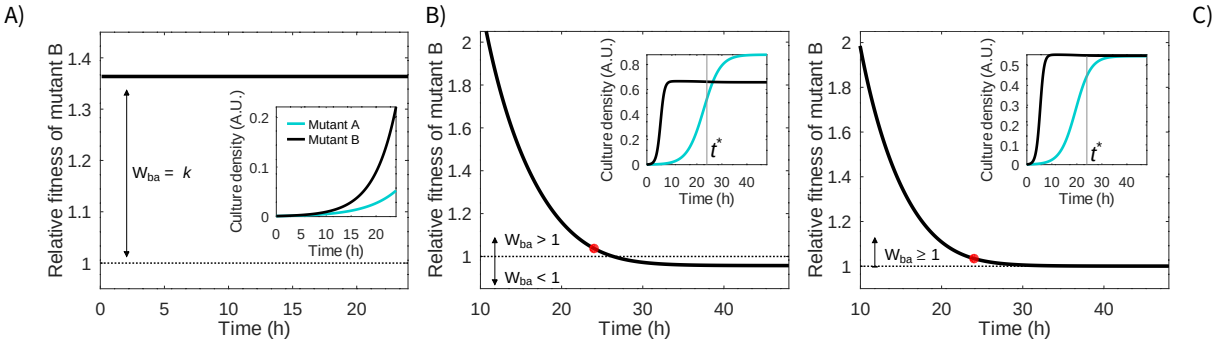

FIGURE 1. Change in relative fitness when populations have exponential and logistic growth. A) Change in relative fitness of mutant B (W_{ba}, black) over time when competing mutants have density-independent, exponential growth—assumed by population genetics theory for populations with continuous growth and overlapping generations (*2*). Relative fitness was calculated as (*5*) $W_{ba} = m_b/m_a$, where m corresponds to the Malthusian parameter for each mutant. The fitness of mutant A, reference, is shown as a black, dotted line. The inset shows the change in cell density, in arbitrary units (A. U.), during the competition. **B-C)** The same information is shown for mutants with density-dependent growth, with (B) and without (C) trade-off between reproduction rate and survival. The sampling time $t^* = 24$ hours, commonly used in microbiological assays, is noted by a red marker in the main plot, and a vertical, grey line in the insets.

is corrected by the term $1-(N_i/K_i)$. Note that I assumed for simplicity that the interference between species is negligible, replacing the Lotka-Volterra competition term (*17*) $1-(N_i-\alpha_j N_j)/K_i$, where $\alpha_j N j$ is the linear reduction in growth rate—in terms of K—of species i by competing species j, for $1-(N_j/K_i)$. This formalisation describes the limitation in growth imposed by the environment, due to finite resources, reducing m over time and leading to density-dependent growth dynamics (Figure 1B and C). In this scenario, m_b depends on the carrying capacity of mutant B, and the relative fitness changes to $W_{ba} = \frac{m_b[1-(B/K_b)]}{m_a[1-(A/K_a)]}$. That is, it can change over time depending on whether the mutants have reached carrying capacity (Figure 1B and C). Now, K_b will determine whether the fitness of mutant B is higher, the same, or indeed lower with respect to mutant A—and *vice versa*—regardless of the value of m_b. In other words, W_{ba} will change through time as genotypes A and B reproduce. When time goes to infinity, the above expression becomes $W_{ba} = K_b/K_a$. Therefore, only when both mutants reach their carrying capacity there will be no further change in densities and, therefore, no further change in fitness.

The fate of new mutants is predicted based on their relative fitness with respect a wild-type genotype (*5, 18, 19*). The fitness of mutant B relative to A as (*5*)

$$W_{ba} = m_b/m_a \tag{3}$$

where W_{ba} is the fitness of mutant B with respect to mutant A, and m the Malthusian parameters for each mutant during the competition. $W_{ba} > 1$ when $m_b > m_a$, that is, when mutant B reproduce faster than mutant A. The expression to calculate m_b experimentally can be derived from the exponential growth model above (*5*)

$$N_b(t) = N_b(0)e^{m_b t} \longrightarrow m_b = ln\left[\frac{N_b(t)/N_b(0)}{t}\right], \tag{4}$$

where $N_b(0)$ is the initial abundance of mutant B, and $N_b(t)$ the abundance of B after an arbitrary period t. Now, it is noteworthy to mention that t is not standardised: If t is too long one competitor may drive the other to extinction, whereas if t is too short the measurement may not be precise (*20*).

Studies that rely on *Escherichia coli* often set $t = 24$ under the assumption that competitors reach the carrying capacity within that time frame (*5*). Unfortunately, growth datasets that validate—or not—this assumption are rarely published. The few that are (*16, 21–23*), however, suggest the assumption is not always met. That is, m can be calculated regardless of whether the genotypes reach carrying capacity (*23*). But does it matter?

Here I simulated a pair-wise competition assay between mutants A and B akin to those used in bacterial evolution. Using the Lotka-Volterra model for competition (*17*), I re-defined the initial conditions of the competition after a growth cycle (c), so that $N_a(c_{+1}, 0) = N_a(c, t^*)d$, $N_b(c_{+1}, 0) = N_b(c, t^*)d$, and $t^* = 24h$ is the time that cells are allowed to grow before propagation. Analog to experimental assays (*22*), each growth cycle has the same duration, and the genotypes are diluted at the beginning of each cycle. Here $0 \leq d \leq 1$ denotes the dilution step.

For haploid populations with continuous growth and overlapping generations and exponential growth, the case assumed by population genetics theory (*1–3*), the mutant reproducing faster—highest m—sweeps to fixation and the mutant reproducing slower—lowest m—is lost (Figure 2A). Regardless of the duration of the growth cycle. Indeed, the only means to reduce differences in fitness in this case is through mutations that increase m. But what if now I apply the same rationale to populations that do not grow exponentially? When the Malthusian parameter is corrected over time due to limited resource availability, then $\mathrm{W_{ba}}$ changes depending on whether the competing genotypes have reached their carrying capacity at the time of propagation. Thus, the outcome of the competition can change depending on the time t^* chosen to propagate the competition as shown in Figures 2B–E). For starters, the mutant with slower reproduction rate is lost *only* if the growth cycles are short enough so that both genotypes are in early growth. Otherwise the genotypes are co-maintained, and the choice of t^* will determine their relative frequencies and whether slow or fast reproducing mutant will be more abundant.

Following the notation of equation 2 above, when $m_a \neq m_b$ and $K_a \approx K_b$ the *perceived* relative fitness of the mutant with faster reproduction rate will be higher ($W_{ba} > W_{ab}$) unless one condition is met: That both reached their carrying capacity when the competition is propagated. In this case, $N_a(t^*) = K_a$ and $N_b(t^*) = K_b$ and therefore $W_{ba} = W_{ab}$. This means that both genotypes can be co-maintained and the mutant reproducing fastest (highest m) is never out-competed (Figure 2B). Now, if the mutant with lower *perceived* relative fitness engages in a trade-off with survival ($m_b > m_a$ and $K_b < K_a$), say, by means of better metabolic efficiency (*12*), this mutant can out-compete its fast-reproducing competitor depending on the choice of t^* (Figure 2C). In other words, the choice of t^* can mislead our conclusions about whether mutant B is beneficial, neutral, or deleterious with respect to A.

Designing protocols that reduce antimicrobial resistance (*24–26*) or plasmid persistence (*27, 28*) rely on accurate fitness measurements. Perhaps more importantly, on the assumption that fitness depends exclusively on genotypes. Mutations (*29*) and acquired plasmids (*30*) that confer resistance against antimicrobials incur fitness costs in the form of either slower growth rate, lower survival or carrying capacity, or lower virulence (*28*). In the case of plasmids, they can be lost rapidly to selection given these costs (*22*). If a plasmid can undergo horizontal gene transfer, it can be maintained provided the conjugation rate is sufficiently high (*31*). If the plasmid is non-transmissible, mutations can reduce—even eliminate—the carriage costs (*22*). However, by the time the mutations occur, only a small fraction of cells can benefit (*22*). Or maybe not?

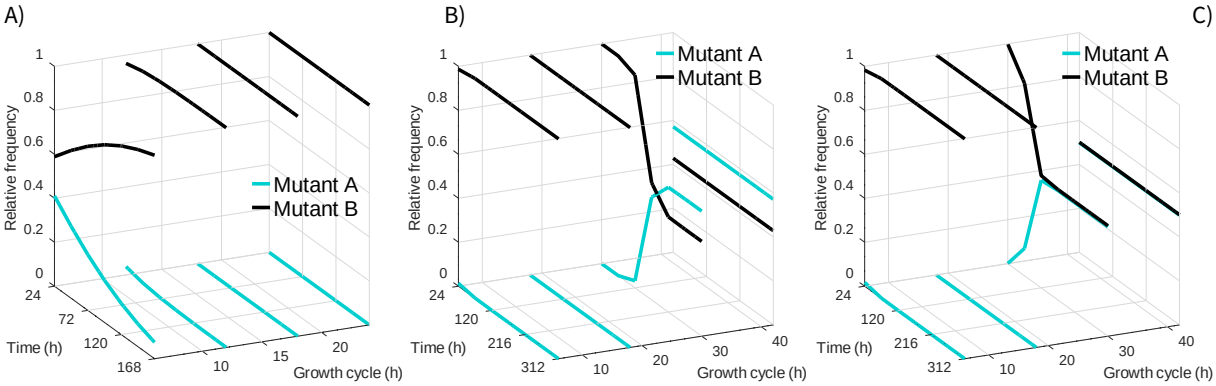

FIGURE 2. Change in relative frequency during competition depending on the length of the growth cycle. Changes in frequency over time for mutants A (cyan) and B (black) following propagations at arbitrary times t=6h, t=12h, t=18h, and t=24h. These times correspond to different stages of growth as Figure 1 shows. Each plot illustrate the case for genotypes with density-independent growth (A), or density-dependent growth where a genotype engages (B) or not (C) in a trade-off between reproduction and survival.

Here I competed two constructs of *Escherichia coli* MC4100, Wyl and GB(c) (see Methods), where I allowed them to reach their carrying capacities. Figure 3A shows this occurs, indeed, within 24 hours. The construct GB(c) carries the non-transmissible plasmid pGW155B (*32*), which harbours *tet(36)*—a ribosome-protection type resistance gene against tetracycline (*32*). The plasmid lacks a *rep* gene to control tightly the partition of plasmids after cell division (*33*–*35*) (addgene vector database accession #2853). While pGW155B is a synthetic plasmid, many natural plasmids also lack partition systems (*35*, *36*). Both constructs have identical chromosome with exception of this plasmid, and the fluorescence gene they carry: Cyan (*cfp*, GB(c)) or yellow (*yfp*, Wyl), to allow their identification in competition assays. Using a non-transmissible plasmid prevents cross-contamination by horizontal gene transfer between the resistant construct GB(c) and Wyl. Importantly, the use of constructs derived from MC4100 avoids interactions between competitors that may affect the outcome of the competition for reasons beyond pGW155B, like the production of bacteriocins (*37*).

Using pure cultures, I found that pGW155B penalised the *per capita* growth rate of construct GB(c) by approximately 40% compared to Wyl (Figure 3B). The duration of lag, and population size were also sensitive to plasmid carriage, regardless of whether I measured the growth using fluorescence or light scattering (Figure S1). Changes in cell size could confound optical density and fluorescence readings, but this phenomenon leaves a signature (*38*) in growth data that is absent in my dataset (Figures S1, S2, and S3). The change in carrying capacity K can be linked to an increase in biomass yield (y) as Monod's expression (*39*) $y = K/s$ suggests, where S the supply of glucose. This metric suggests that construct GB(c) is more efficient than Wyl (Figures 3B and C), which is not surprising given that GB(c) also synthesises proteins encoded by the plasmid with the same supply of glucose. This means that pGW155B triggers a metabolic trade-off between growth rate and carrying capacity (*11*, *12*).

For the competition assay, I mixed equal proportions—cell to cell—of two pure cultures, from construct GB(c) and Wyl respectively, grown overnight, in media containing no antibiotic or 0.04 µg/mL of tetracycline (see Methods). I incubated the mixed culture at 30°C until both constructs reached their carrying capacity (K, ~ 24h as per data in Figure 3A), and then I propagated the competition into a new plate containing fresh media. I repeated the propagation step seven times. Indeed, the relative fitness of both constructs changed through time. In the presence of tetracycline

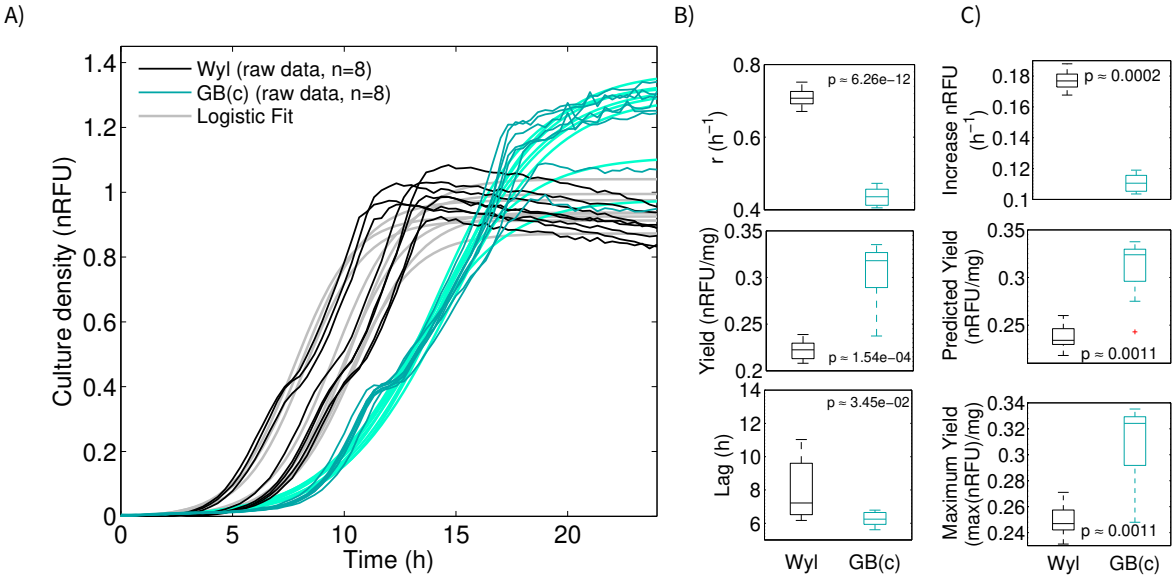

Figure 3. Asymmetric carriage costs of pGW155B. A) Overlapped growth curves of constructs Wyl (black) and GB(c) (cyan) in the absence of tetracycline over 24h. I estimated the growth rate *per capita* (r), population size in the equilibrium (K), biomass yield, and lag duration from a 4-parameter logistic model fitted to growth data (see Methods). Data fits for constructs Wyl and GB(c) are shown in grey and light cyan, respectively. **B)** Box plots showing the median (centre of the box), 25th and 75th percentile for each of the aforementioned parameters. The whiskers extend to the most extreme data points that are not outliers, and these are individually represented. The *p* value shown refers to a Two-sample *t*-test with unequal variance (8 replicates) that I used to test differences in the parameters between both constructs. **C)** Alternative metrics for growth rate and biomass yield: Forward Euler approximation (top), data fit predicted yield (middle), and maximal yield across all time points in growth data (bottom). The *p* values correspond to Two-sample *t*-tests with unequal variance (8 replicates).

the relative fitness of drug-sensitive construct Wyl was below GB(c), which harbours pGW155B, at all times as Figure 4A illustrates. This meant that GB(c) increased its relative frequency in following propagation steps and became the most abundant construct throughout the competition (Figure 4B). During the competition, the number of copies of pGW155B harboured by GB(c) increased 5- to 6-fold driven by exposure to tetracycline (2-sample *t*-test with unequal variances, $p = 0.0088$, $df = 2.5826$, *t*-statistic= -7.2441; with 3 replicates. Figure 4C).

Without tetracycline, however, the relative fitness of Wyl can be higher, equal, or lower than construct GB(c) at different times as Figure 4D shows. This meant that when I propagated the competition, after 24h of growth, the relative frequency of Wyl remained below GB(c) despite its faster growth rate (Figure 4E). Or, in other words, plasmid-harbouring construct GB(c) out-competed its plasmid-free competitor despite its slower growth rate. Surprisingly, I found no substantial variation in the number of copies of pGW155B borne by this construct despite the lack of exposure to tetracycline (2-sample *t*-test with unequal variances, $p = 0.2305$, $df = 2.2351$, *t*-statistic= -1.6353; with 3 replicates. Figure 4F). This contrasts with previous studies (*22*) showing the rapid decline, within a similar time frame, in bacteria harbouring non-transmissible plasmids.

III. Discussion

Here I showed that conventional fitness measurements in microbial populations, which rely on Fisher's rationale, will change through time without requiring any mutations. This means that protocols, or indeed policies based on fitness assays can be potentially misleading: Mutants that were

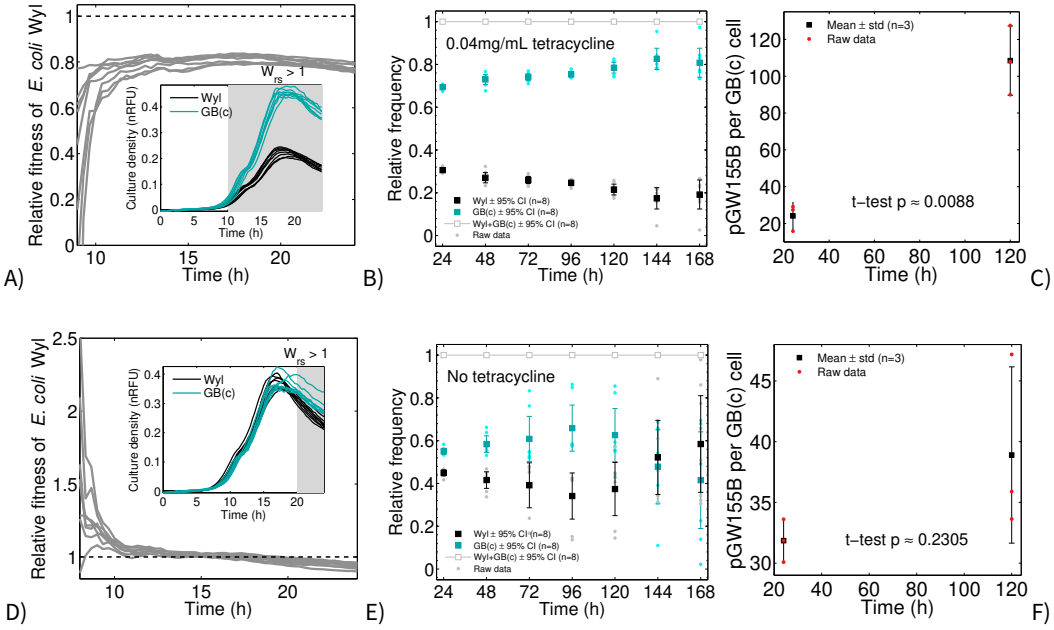

FIGURE 4. Time-dependent fitness data allows co-maintenance of both constructs without tetracycline. Relative fitness during first 24 hour pairwise-competition of construct Wyl, where both constructs grew in media supplemented with 0.04 µg/mL of tetracycline (**A**) and without drug (**D**). Fitness for each replicate is presented with respect to the reference GB(c) (black dashed line). The inset illustrate the growth curves for both constructs, highlighting in grey the period where the relative fitness of Wyl (W_{sr}) is lower than its tetracycline-resistant competitor's. **B)** and **E)** show the change in relative frequency of both constructs through time when both constructs grew in media supplemented with tetracycline (B) and without antibiotic (E). Error bars represent the mean ± 95% confidence intervals, with raw data points shown as dots. **C)** and **F)** show the change in relative copy numbers of pGW155B borne by construct GB(c) during the pairwise-competition, calculated using quantitative PCR (see Methods). Error bars represent the mean ± standard deviation, with raw data shown in red.

predicted to be lost can be maintained depending on when fitness was measured, and whether these mutants engage in trade-offs. This have both practical and academic implications. For example, antimicrobial-resistant mutants incur 'fitness cost' (*19, 24–26, 40*) grow slower than their sensitive counterparts. Conventional wisdom holds that withdrawal of antimicrobials should therefore reduce the prevalence of antimicrobial resistance, but this prediction does not seem consistent with available clinical data (*41–44*). My study can help understand why.

Similar rationale can be applied to plasmid carriage and their seemingly-paradoxical (*30*) abundance in nature. While the abundance of plasmids able to undergo horizontal gene transfer can be explained through high conjugation rates (*31*), most of the known plasmids are unable to do this (*45*). Here I argue that classical fitness competition assays can confound carriage costs because they do not allow microorganisms reach their equilibrium. Indeed, data (*23*) suggest that so-called 'plasmid benefits' occur only during the latest hours of these assays, meaning more plasmids could show them if allowed to reach their equilibrium. In other words, plasmids may not be as costly as previously thought, which can explain why they are so abundant.

Population genetics theory proposes abstract mathematical models to understand how populations evolve, but they are rarely tested in the laboratory (*46, 47*). Microbial populations offer an excellent opportunity to test them and contribute to a better understanding of natural selection—which can have academic and policy-making implications.

Competing interests

The author declares no competing interests.

Acknowledgements

The author thanks Robert Beardmore for laboratory support.

IV. Methods

Media and Strains. I used the strains of *Escherichia coli* GB(c) and Wyl (*48*) (a gift from Remy Chait and Roy Kishony), and M9 minimal media supplemented with 0.4% glucose and 0.1% casamino acids (w/v). I made tetracycline stock solutions from powder stock (Duchefa, Ref. #0150.0025) at 5mg/mL in 50% ethanol, filter sterilised, and stored at -20^oC. Subsequent dilutions were made from this stock in supplemented M9 minimal media and kept at 4^oC.

Batch transfer protocol. I inoculated a 96-well microtitre plate containing 150µg/mL of supplemented M9 media with a mixture of two overnight cultures, one of *E. coli* GB(c) and another of *E. coli* Wyl (Figure S2). The overnight culture for GB(c) was supplemented with 100ng/mL of tetracycline to preserve the plasmid pGW155B carrying *tet(36)* as described elsewhere (*13*), then centrifuged and removed prior adding to the microtitre plate. I incubated the plate at 30^oC in a commercial spectrophotometer and measured the optical density of each well at 600nm (OD_{600}), yellow florescence for the Wyl strain (YFP excitation at 505nm, emission at 540nm), and cyan fluorescence for the GB(c) strain (CFP at 430nm/480nm) every 20min for 24h. After each day I transferred 1.5µL of each well, using a 96-well pin replicator, into a new microtitre plate containing fresh growth medium and tetracycline.

Growth parameter estimation. Yellow and cyan fluorescence protein genes were constitutively expressed given the constant ratio between fluorescence and optical density (Figure S4). This allowed me to use fluorescence data as a proxy for cell density in mixed culture conditions. I normalised fluorescence readings using a conversion factor, n_f, calculated by growing each construct in a range of glucose concentrations, and regressing the linear model $RFU = n_f \cdot OD + c$ where RFU is relative fluorescence units data, OD optical density data, n_f the conversion factor between fluorescence and optical density, and c the crossing point with the y–axis when $OD = 0$. I imported the resulting time series data set (Figures S3) into `MATLAB R2014b` to subtract background and calculate fitness as described in the main text.

DNA material extraction. For each concentration, I sampled three representative 150µg/mL replicates that I divided into two groups for chromosome and plasmid DNA extraction. I used 'GeneJet DNA' (ThermoScientific, Ref. #K0729) and 'GeneJet Plasmid' (ThermoScientific, Ref. #K0502) extraction kits to extract chromosomal and plasmid DNA (pDNA) from the samples, respectively, and used Qubit to quantify DNA and pDNA yields. Both extracts were diluted accordingly in extraction buffer, as per in manufacturer instructions, to normalise DNA across samples.

Quantitative PCR and plasmid copy number estimation. I used `primer3` to design two pairs of primers with melting temperature (T_m) of 60°C and non-overlapping probes with T_m of 70°C. The amplicon ranges between 100 to 141bp depending on the locus (Table 1). Two reaction mixes were prepared using the kit 'Luminaris Color Probe Low ROX' (ThermoScientific, Ref. #K0342), adding 0.3µM of each primer and 0.2µM of the probe as per manufacturer specifications. Following a calibration curve for each reaction (Figure S5) I added 0.01ng of chromosomal or plasmid DNA material to each of the reaction mixes.

Table 1. Primers and probes designed using `Primer3`. Amplicon ranging from 100 to 141bp. T_m indicates the estimated melting temperature.

Target gen	Sequence ($5' \rightarrow 3'$)	T_m (^{o}C)	Feature
tatB	CGATGAAGCGTTCCTACGTT	60.27	Forward
	TCATGCGCAGCTTCATTATC	59.94	Reverse
	AAGGCGAGCGATGAAGCGCA	70.70	Probe
tet(36)	ATTGGGCATCTATTGGCTTG	59.22	Forward
	CCGATTCACAGGCTTTCTTG	60.76	Reverse
	AGCCTTTGCCAATTGGGGCG	70.37	Probe

To estimate the relative copies of pGW155B per GB(c) cell, I calculated the corresponding proportion of chromosomal DNA corresponding to the GB(c)-type from data in Figure **??**D and used the expression (*22*)

$$cn = \frac{(1+E_c)^{Ctc}}{(1+E_p)^{Ctp}} \times \frac{S_c}{S_p},$$

where cn is the number of plasmid copies per chromosome, S_c and S_p are the size of the chromosome and pGW155B amplicon in bp, E_c and E_p the efficiency of the qPCR taken from data in Figure S5, and Ctc and Ctp are the cycles at which I first detected product amplification (C_t).

REFERENCES

1. Fisher, R. A. *The Genetical Theory of Natural Selection* 308–315 (At The Clarendon Press, 1930).
2. Crow, J. F., Kimura, M., *et al. An introduction to population genetics theory.* (New York, Evanston and London: Harper & Row, Publishers, 1970).
3. Templeton, A. *Population Genetics and Microevolutionary Theory* ISBN: 9780471409519 (Wiley, 2006).
4. Orr, H. A. Fitness and its role in evolutionary genetics. *Nat. Rev. Genet.* **10,** 531–539 (2009).
5. Lenski, R. E., Rose, M. R., Simpson, S. C. & Tadler, S. C. Long-Term Experimental Evolution in Escherichia coli. I. Adaptation and Divergence During 2,000 Generations. *Am. Nat.* **138,** pp. 1315–1341 (1991).
6. Wiser, M. J., Ribeck, N. & Lenski, R. E. Long-term dynamics of adaptation in asexual populations. *Science* **342,** 1364–1367 (2013).
7. Kassen, R. & Bataillon, T. Distribution of fitness effects among beneficial mutations before selection in experimental populations of bacteria. *Nat. Genet.* **38,** 484–488 (2006).

8. Ghoul, M. & Mitri, S. The ecology and evolution of microbial competition. *Trends Microbiol.* **24,** 833–845 (2016).

9. Pope, C. F., McHugh, T. D. & Gillespie, S. H. in *Antibiotic Resistance Protocols* 113–121 (Springer, 2010).

10. Ferenci, T. Trade-off mechanisms shaping the diversity of bacteria. *Trends Microbiol.* **24,** 209–223 (2016).

11. Reznick, D., Bryant, M. J. & Bashey, F. r-and K-selection revisited: the role of population regulation in life-history evolution. *Ecology* **83,** 1509–1520 (2002).

12. Reding-Roman, C., Hewlett, M., Duxbury, S., *et al.* The unconstrained evolution of fast and efficient antibiotic-resistant bacterial genomes. *Nat. Ecol. Evol.* **1,** 0050 (2017).

13. Chait, R., Craney, A & Kishony, R. Antibiotic interactions that select against resistance. *Nature* **446,** 668–671 (2007).

14. Wang, H., Avican, K., Fahlgren, A., *et al.* Increased plasmid copy number is essential for Yersinia T3SS function and virulence. *Science* **353,** 492–495 (2016).

15. Adkar, B. V., Manhart, M., Bhattacharyya, S., *et al.* Optimization of lag phase shapes the evolution of a bacterial enzyme. *Nat. Ecol. Evol.* **1,** 1–6 (2017).

16. Concepción-Acevedo, J., Weiss, H. N., Chaudhry, W. N. & Levin, B. R. Malthusian parameters as estimators of the fitness of microbes: a cautionary tale about the low side of high throughput. *PLoS One* **10,** e0126915 (2015).

17. Gilpin, M. E. & Ayala, F. J. Global models of growth and competition. *Proc. Natl. Acad. Sci. U.S.A.* **70,** 3590–3593 (1973).

18. Svara, F. & Rankin, D. J. The evolution of plasmid-carried antibiotic resistance. *BMC Evol. Biol.* **11,** 130 (2011).

19. Day, T., Huijben, S. & Read, A. F. Is selection relevant in the evolutionary emergence of drug resistance? *Trends Microbiol.* **23,** 126–133 (2015).

20. McDonald, M. J. Microbial experimental evolution–a proving ground for evolutionary theory and a tool for discovery. *EMBO Rep.* **20,** e46992 (2019).

21. Keymer, J. E., Galajda, P., Lambert, G., Liao, D. & Austin, R. H. Computation of mutual fitness by competing bacteria. *Proc. Natl. Acad. Sci. U.S.A.* **105,** 20269–20273 (2008).

22. Millán, A. S., Peña-Miller, R., Toll-Riera, M, *et al.* Positive selection and compensatory adaptation interact to stabilize non-transmissible plasmids. *Nat. Commun.* **5** (2014).

23. Alonso-del Valle, A., León-Sampedro, R., Rodríguez-Beltrán, J., *et al.* Variability of plasmid fitness effects contributes to plasmid persistence in bacterial communities. *Nat. Commun.* **12,** 1–14 (2021).

24. Bonhoeffer, S, Lipsitch, M & Levin, B. R. Evaluating treatment protocols to prevent antibiotic resistance. *Proc. Natl. Acad. Sci. U.S.A.* **94,** 12106–11 (Oct. 1997).

25. Bergstrom, C. T., Lo, M. & Lipsitch, M. Ecological theory suggests that antimicrobial cycling will not reduce antimicrobial resistance in hospitals. *Proc. Natl. Acad. Sci. U.S.A.* **101,** 13285–90 (2004).

26. Wang, Y. C. & Lipsitch, M. Upgrading antibiotic use within a class: tradeoff between resistance and treatment success. *Proc. Natl. Acad. Sci. U.S.A.* **103,** 9655–9660 (2006).

27. Bergstrom, C. T., Lipsitch, M. & Levin, B. R. Natural selection, infectious transfer and the existence conditions for bacterial plasmids. *Genetics* **155,** 1505–1519 (2000).

28. Vogwill, T. & MacLean, R. C. The genetic basis of the fitness costs of antimicrobial resistance: a meta-analysis approach. *Evol. Appl.* **8,** 284–295 (2015).

29. Andersson, D. I. & Levin, B. R. The biological cost of antibiotic resistance. *Curr. Opin. Microbiol.* **2,** 489–493 (1999).

30. Harrison, E. & Brockhurst, M. A. Plasmid-mediated horizontal gene transfer is a coevolutionary process. *Trends Microbiol.* **20,** 262–267 (2012).

31. Lopatkin, A. J., Meredith, H. R., Srimani, J. K., *et al.* Persistence and reversal of plasmid-mediated antibiotic resistance. *Nat. Commun.* **8,** 1689 (2017).

32. Whittle, G, Whitehead, T. R., Hamburger, N, Shoemaker, N. B., Cotta, M. A., *et al.* Identification of a new ribosomal protection type of tetracycline resistance gene, tet(36), from swine manure pits. *Appl. Environ. Microbiol.* **64,** 4151–4158 (2003).

33. Del Solar, G. & Espinosa, M. Plasmid copy number control: an ever-growing story. *Mol. Microbiol* **37,** 492–500 (2000).

34. Garcillán-Barcia, M. P., Alvarado, A. & de la Cruz, F. Identification of bacterial plasmids based on mobility and plasmid population biology. *FEMS Microbiol. Rev.* **35,** 936–956 (2011).

35. Million-Weaver, S. & Camps, M. Mechanisms of plasmid segregation: have multicopy plasmids been overlooked? *Plasmid* **75,** 27–36 (2014).

36. Guynet, C. & de la Cruz, F. Plasmid segregation without partition. *Mob. Genet. Elements* **1,** 236–241 (2011).

37. Dobson, A., Cotter, P. D., Ross, R. P. & Hill, C. Bacteriocin Production: a Probiotic Trait? *Appl. Environ. Microbiol.* **78,** 1–6 (2012).

38. Stevenson, K., McVey, A. F., Clark, I. B., Swain, P. S. & Pilizota, T. General calibration of microbial growth in microplate readers. *Sci. Rep.* **6,** 1–7 (2016).

39. Monod, J. *Recherches sur la croissance des cultures bactériennes* PhD thesis (Paris, 1941).

40. Basra, P., Alsaadi, A., Bernal-Astrain, G., *et al.* Fitness tradeoffs of antibiotic resistance in extraintestinal pathogenic Escherichia coli. *Genome Biol. Evol.* **10,** 667–679 (2018).

41. McGowan, J. E. Minimizing antimicrobial resistance in hospital bacteria: can switching or cycling drugs help? *Infect. Control Hosp. Epidemiol.* **7,** 573–576 (1986).

42. Brown, E. M. & Nathwani, D. Antibiotic cycling or rotation: a systematic review of the evidence of efficacy. *J. Antimicrob. Chemother.* **55,** 6–9 (2005).

43. Böttger, E. C., Pletschette, M. & Andersson, D. Drug resistance and fitness in Mycobacterium tuberculosis infection. *J. Infect. Dis.* **191,** 823–824 (2005).

44. Böttger, E. C. & Springer, B. Tuberculosis: drug resistance, fitness, and strategies for global control. *Eur. J. Pediatr.* **167,** 141–148 (2008).

45. Smillie, C., Garcillán-Barcia, M. P., Francia, M. V., Rocha, E. P. & de la Cruz, F. Mobility of plasmids. *Microbiol. Mol. Biol. Rev.* **74,** 434–452 (2010).

46. Wakeley, J. The limits of theoretical population genetics. *Genetics* **169,** 1–7 (2005).

47. Orr, H. A. The population genetics of beneficial mutations. *Philos. Trans. R. Soc. Lond., B, Biol. Sci.* **365,** 1195–1201 (2010).

48. Chait, R., Shrestha, S., Shah, A. K., Michel, J.-B. & Kishony, R. A Differential Drug Screen for Compounds That Select Against Antibiotic Resistance. *PLoS One* **5,** e15179 (2010).

I. Supplementary Figures

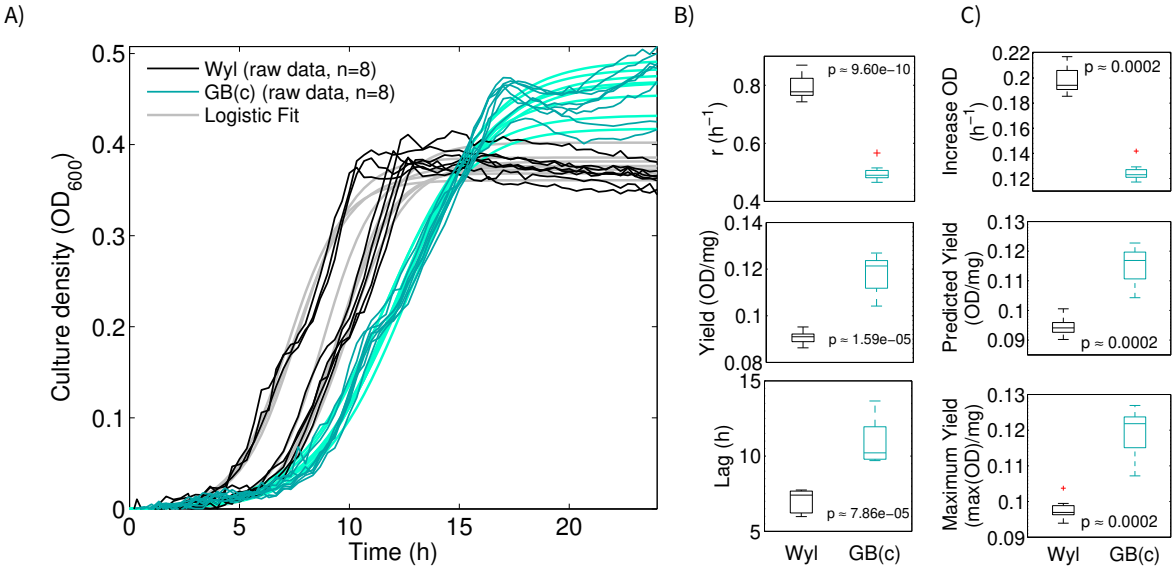

Figure S1. Asymmetric carriage costs of pGW155B (optical density data). A) Overlapped growth curves of constructs Wyl (black) and GB(c) (cyan) in the absence of tetracycline over 24h. I estimated the growth rate *per capita* (r), population size in the equilibrium (K), biomass yield, and lag duration from a 4-parameter logistic model fitted to growth data (see Methods). Data fits for constructs Wyl and GB(c) are shown in grey and light cyan, respectively. **B)** Box plots showing the median (centre of the box), 25th and 75th percentile for each of the aforementioned parameters. The whiskers extend to the most extreme data points that are not outliers, and these are individually represented. The *p* value shown refers to Two-sample *t*-tests with unequal variance (8 replicates) that I used to test differences in the parameters between both constructs. **C)** Alternative metrics for growth rate and biomass yield: Forward Euler approximation (top), data fit predicted yield (middle), and maximal yield across all time points (bottom). The *p* values correspond to Two-sample *t*-tests with unequal variance (8 replicates).

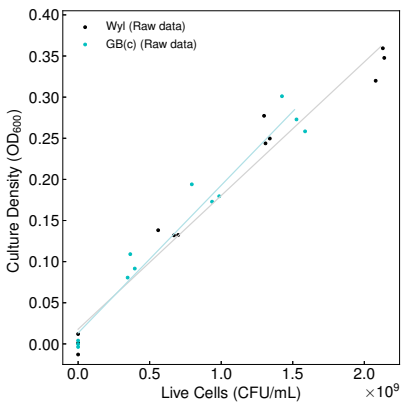

Figure S2. Calibration curve to translate optical density data to number of *Escherichia coli* cells. I fitted the linear model $a = bx + c$ to optical density and colony counting data (dots) to calculate the number of optical density units (OD_{600}) per cell. a denotes the optical density readings measured at 600nm, c the crossing point with the $y-$axis when $x = 0$, and b the conversion factor between optical density and number of cells (x). I interpolating optical density readings to calculate the number of cells within a culture as $x = (a - c)/b$. For the strain Wyl, $b = 1.62 \times 10^{-10}\ OD \cdot mL \cdot CFU^{-1}$ and $c = 1.78 \times 10^{-2}\ OD$, whereas for GB(c) $b = 1.79 \times 10^{-10}\ OD \cdot mL \cdot CFU^{-1}$ and $c = 1.33 \times 10^{-2}\ OD$.

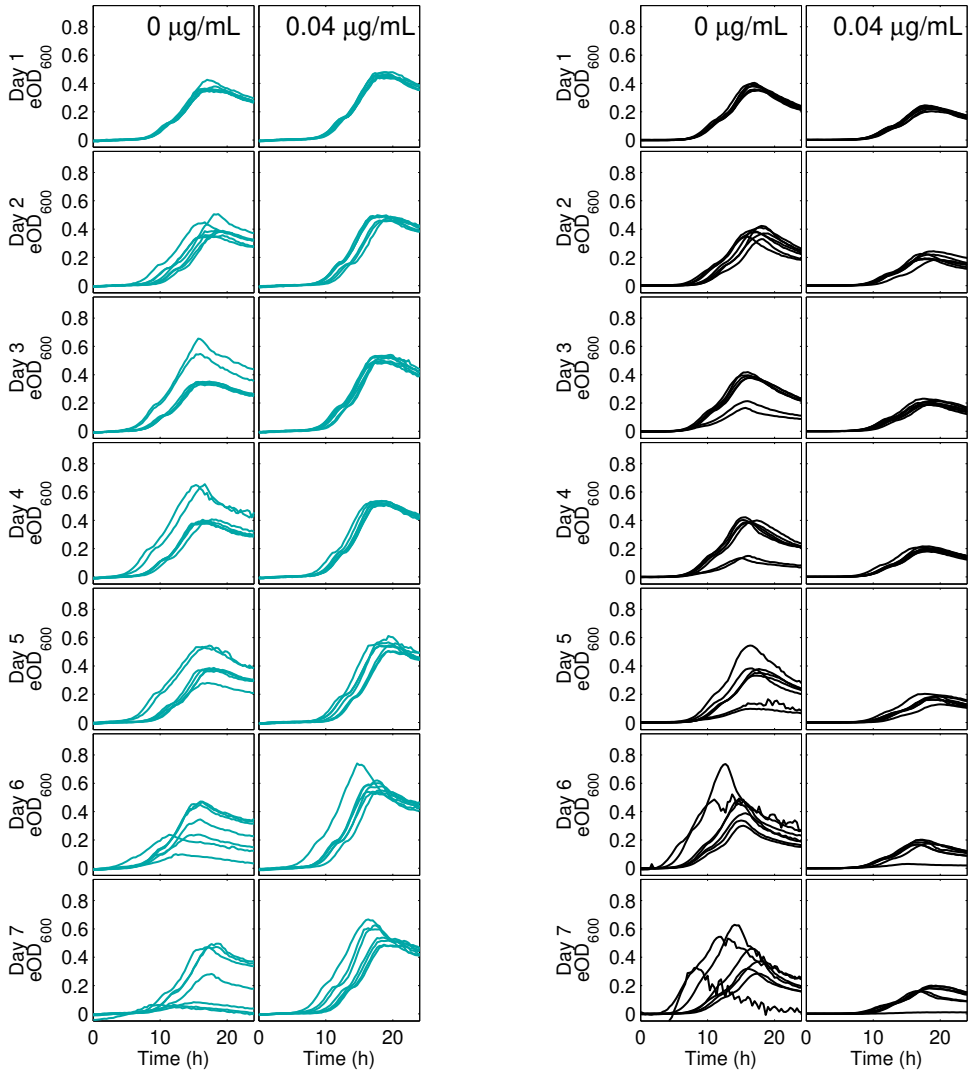

FIGURE S3. Raw data of each construct during the competition. Raw optical density data for GB(c) (cyan) and Wyl (black), measured every 20 min and converted from fluorescence readings. Each individual plot represents the change in abundance of each construct over 24 hours. Data corresponding to each condition, with and without tetracycline, are aggregated as columns.

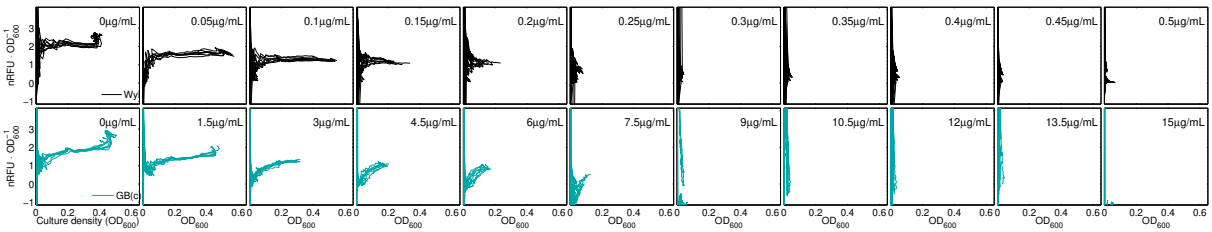

FIGURE S4. Changes in relative fluorescence over time in GB(c) and Wyl strains in pure culture conditions. Raw change in florescence, per optical density units, measured every 20min for 24h for the Wyl- (black) and GB(c)-type. Each column represents the data set for each tetracycline concentration used.

A) B)

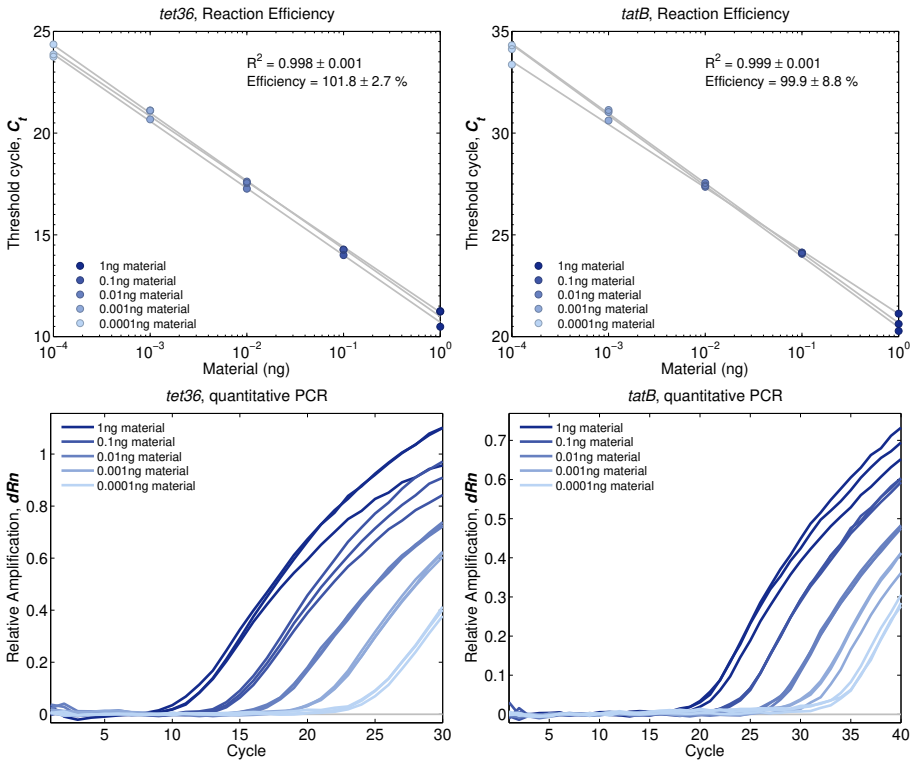

C) D)

Figure S5. Quantitative PCR calibration curves for *tet(36)* and *tatB*. Reaction efficiency for the set of primers and probes, listed in Table 1 the main Methods section, for *tet(36)* (A) and *tatB*. The efficiency was calculated as $E_f = 10^{-1/Slope} - 1$, and the slope term calculated by fitting a linear model to qPCR threshold cycle (C_t) data. The mean ± standard deviation for the adjusted coefficient of determination R^2 and efficiency are shown in the figures. The amplification curves for each reaction, using 3 replicates, are shown in C) and D), respectively.